J. Am. Chem. Soc. 1989, 111, 3819-3824

Mass-Mobility Correlation of Ions in View of New Mobility Data

Zvi Berant and Zeev Karpas*

Contribution from the Physics Department, Nuclear Research Center, Negev, P.O. Box 9001, Beer-Sheva, Israel 84190. *Received April 11, 1988*

Abstract: The reduced mobility of the major ion formed in aliphatic amines, aromatic amines, and acetyls was determined by ion mobility spectrometry (IMS) techniques. This acquisition of a large amount of data on the mobility of polyatomic ions in air and helium, under low E/N conditions, enabled us to take a fresh view on the agreement between theory and experiment. Models based on the rigid sphere or the polarization limit approximations do not properly represent the interaction between the ion and drift gas molecules. Use of Mason's model with a hard-core potential qualitatively reproduced experimental data, although quantitative agreement over a broad range of ion masses, especially in helium, was only fair. Better quantitative agreement was obtained when the model was slightly modified, by introduction of an empirical mass-dependent correction term in the collision cross-section term. This was done through the expression for the position of the minimum in the interaction potential, r_m; $r_m = (r_o + zm)[1 + (m/M)^{1/3}]$, where z is the correction term.

It is important to estimate the mobility of ions in air and other gases for several applications, such as rate determination of ionic processes in the atmosphere, calculation of the electric conductivity of gases, and analytical purposes based on ion mobility spectrometry (IMS). Although measurements of ion mobilities and theoretical models to interpret them abound, there is a need for a systematic experimental study and especially for a critical evaluation of the suitability of these models for polyatomic ions.

In the present work, the mobilities in an electric field of several polyatomic ions, belonging to three families of compounds, were measured by the IMS method. The experimental data obtained were analyzed in view of some commonly used theoretical models. The effect on the mobility of changing the drift gas from air to helium was also examined.

1. Theory of Ion Mobility. The theoretical foundations dealing with the mobility of ions in an electric field date back to Langevin,[1] whose model took into consideration only ion-induced dipole interactions. Advances in theoretical understanding, accompanied by accumulation of experimental data, have brought some refinements to the original theory. Extensive discussions on the subject can be found in the literature.[2-7] Especially helpful is the review by Mason,[3] one of the major contributors to the field.

Basically, the formula for the mobility, K, is

$$K = (3q/16N)(2\pi/\mu kT_{\mathrm{eff}})^{1/2}[(1 + \alpha)/\Omega_D(T_{\mathrm{eff}})] \qquad (1)$$

where the reduced mass is $\mu = mM/(m + M)$; q is the ion charge and m its mass; N is the density of the neutral molecules and M their mass; k is the Boltzmann constant; Ω_D is the ion–neutral cross section; and α is a correction term, generally less than 0.02 for $m \geq M$ (ref 3, p 50), and therefore set to zero. T_{eff} is the effective temperature of the ions. The sophisticated approach to the question of ion temperature, presented by Viehland,[7] was not adopted here because of the low E/N (about 1 Td $\equiv 10^{-17}$ V cm^2) in the IMS cell, which makes T_{eff} essentially equal to the cell temperature.[3] The mass dependence of the mobility enters through μ and Ω_D. Evidently, for heavy ions drifting through light neutral molecules the reduced mass will be practically invariable with the ion mass.

The collision cross-section term, Ω_D, contains all the information on the interaction between the ion and molecule, namely, the nature of the interaction, like ion–dipole, ion-induced dipole, etc. Following the treatment of ref 3

$$\Omega_D = \pi r_m^2 \Omega^{(1,1)*}(T^*) \qquad (2)$$

where, $\Omega^{(1,1)*}(T^*)$ is the dimensionless collision integral that depends on the ion–neutral interaction potential and is a function of the dimensionless temperature, $T^* = kT/\epsilon_0$. Here, ϵ_0 is the depth of the potential minimum and r_m its position. ϵ_0 was calculated from $\epsilon_0 = (e^2\alpha_p/[3r_m^4(1 - a^*)^4]$ (eq 5 in ref 11), where α_p and a^* are as defined below.

By making simplified assumptions on the nature of these interactions, the collision cross section can be estimated for some special cases. One approach treats the ion and neutral molecule as rigid spheres, and the collision cross-section term that appears in eq 1 is simply

$$\Omega_D = \pi(r_i + r_N)^2 \qquad (3)$$

where r_i and r_N are the radii of the ion and neutral molecule, respectively.

In the polarization limit approach it is assumed that the molecule has no permanent dipole or quadrupole moments, and the only interaction arises from the ion-induced dipole potential. This depends on the polarizability of the neutral, α_p. In the limit where the electric field $E \rightarrow 0$ and the temperature $T \rightarrow 0$, the collisional cross section is proportional to $(q^2\alpha_p/kT)^{1/2}$, and the mobility is[3]

$$K_{\mathrm{pol}} = 13.853/(\alpha_p\mu)^{1/2} \qquad (4)$$

The assumptions underlying both the above approaches limit their applicability. They have been used with limited success in some cases where small, generally monoatomic, ions drift through a neutral, in most cases inert, gas, such as helium (see section 2.3.1 of ref 3). However, the failure of these models to quantitatively explain mobility data has been demonstrated time and again (for example, see ref 8). As shown below, the rigid sphere model can be used to reproduce the experimental data over a limited range of ion masses.

Our interest lies in the study of polyatomic ions[9,10] where the oversimplifications inherent in both these treatments render them

---

(1) Langevin, P. *Ann. Chim. Phys.* **1905**, *5*, 245. An English translation appears in Appendix II of: *Collision Phenomena in Ionized Gases*; McDaniel, E. W., Ed.; Wiley: New York, 1984.

(2) McDaniel, E. W.; Mason, E. A. *The Mobility and Diffusion of Ions in Gases*; Wiley-Interscience: New York, 1973.

(3) Mason, E. A. In *Plasma Chromatography*; Carr, T. W., Ed.; Plenum Press: New York, 1984; Chapter 2.

(4) Revercomb, H. E.; Mason, E. A. *Anal. Chem.* **1975**, *47*, 970.

(5) (a) Ellis, H. W.; Pai, R. Y.; McDaniel, E. W.; Mason, E. A.; Viehland, L. A. *At. Nucl. Data Tables* **1976**, *17*, 177. (b) Ellis, H. W.; McDaniel, E. W.; Albritton, D. L.; Viehland, L. A.; Lin, S. L.; Mason, E. A. *Ibid.* **1978**, *22*, 179. (c) Ellis, H. W.; Thackston, M. G.; McDaniel, E. W.; Mason, E. A. *Ibid.* **1984**, *31*, 113.

(6) Parent, D. C.; Bowers, M. T. *Chem. Phys.* **1981**, *60*, 257.

(7) (a) Viehland, L. A.; Lin, S. L. *Chem. Phys.* **1979**, *43*, 135. (b) Viehland, L. A.; Fahey, D. W. *J. Chem. Phys.* **1983**, *78*, 435.

(8) Bohringer, H.; Fahey, D. W.; Lindinger, W.; Howorka, F.; Fehsenfeld, F. C.; Albritton, D. L. *Int. J. Mass Spectrom. Ion Proc.* **1987**, *81*, 45.

(9) (a) Karpas, Z.; Cohen, M. J.; Stimac, R. M.; Wernlund, R. F. *Int. J. Mass Spectrom. Ion Proc.* **1986**, *74*, 153. Karpas, Z.; Stimac, R. M.; Rappoport, Z. *Ibid.* **1988**, *83*, 163.

(10) Karpas, Z., submitted for publication in *Anal. Chem.*

0002-7863/89/1511-3819$01.50/0

ineffective. We shall therefore turn to a short discussion of the mobility formula, eq 1, in conjunction with the hard-core potential. A detailed treatment can be found elsewhere.[2,3]

As we are dealing with relatively large, complex polyatomic ions, it can no longer be assumed that the center of mass of the ion is also the center of its charge. Therefore a parameter a, the effective core diameter[3,11] which expresses the separation of these centers, is introduced. The interaction potential for the most commonly treated case, the so-called 12,4 or hard-core potential,[2,3,5,6] becomes

$$V(r) = (\epsilon_0/2)\{[(r_m - a)/(r - a)]^{12} - 3[(r_m - a)/(r - a)]^4\} \qquad (5)$$

where, ϵ_0 and r_m are as defined above. It is more convenient to use a reduced core diameter, $a^* \equiv a/r_m$. The drift time of a singly charged ion ($q = e$), which is proportional to the inverse mobility, K^{-1}, depends on its mass (through $\mu^{1/2}$) and on the collision cross section. As mentioned above, for heavy ions in a light gas, μ is nearly constant, and the mobility is therefore controlled, at a given temperature, by Ω_D. It can reasonably be assumed that the ion radius in a homologous series varies as the cubed root of its mass.[3] Thus, r_m can be expressed as

$$r_m = r_0[1 + b(m/M)^{1/3}] \qquad (6)$$

where b is a constant representing the relative density of ion and neutral reactants and was set to unity, and r_0 is a constant. As seen in eq 2, the collision cross section depends on r_m^2, so that the relative mobility of ions in a homologous series of compounds should follow a simple correlation.[12]

The reduced mobility can therefore be calculated from a modified form of eq 1, in which the appropriate constants and units were substituted to give 1.697×10^{-4}:

$$K_0^{-1} = 1.697 \times 10^{-4}(\mu T)^{1/2} r_m^2[\Omega^{(1,1)*}(T^*)] \qquad (7)$$

where, T^* and $\Omega^{(1,1)*}$ are as defined above. The units of K_0 are cm^2 V^{-1} s^{-1} if the masses are expressed in atomic mass units, r_0 in Ångstroms, and T in degrees Kelvin. Extensive use of the relationship between the ion mass and the mobility in air and in helium was made, using eq 7. However, the experimental data points, especially in helium, could not be satisfactorily reproduced by using this equation. It was found empirically that modifying the expression for r_m given by eq 6, by introducing an additional mass-dependent term (eq 8), greatly improved agreement between the calculated and measured reduced mobilities

$$r_m = (r_0 + zm)[1 + (m/M)^{1/3}] \qquad (8)$$

where z, the correction factor, is a constant. Throughout the next sections, this modified expression is used in the calculations based on eq 7.

2. Compounds Studied. In order to determine the mass-mobility correlation for a large, yet internally consistent, series of polyatomic ions, three families of compounds were studied. These were substituted aliphatic amines, aromatic amines (anilines and pyridines), and acetyls. Some of the ions contain a saturated hydrocarbon chain with only a single substituent heteroatom, some have up to four such atoms, and in others there are unsaturated hydrocarbon chains or rings. Thus, the relative density of the ions should somewhat vary.

As shown by IMS/MS studies,[10] these compounds share an important common feature as they protonate readily in the IMS source and yield the protonated molecule as the major ionic species. Some exceptions were noted previously and were taken into account when the mass-mobility correlations were investigated. For example, quaternary amines lose a RX group (X = OH or halide), yielding the protonated tertiary amine as the major ionic species, and tertiary amines may fragment to lower amines.[10]

The aromatic amines can be viewed as having a rigid carbon skeleton, the aromatic system, which is barely affected by protonation or substitution, while the acetyls and aliphatic amines can be regarded as more volatile structures. Anilines may protonate on the nitrogen, leaving the aromatic system intact, or on the aromatic ring.[13] Also, the site of protonation in acetyls is on the carbonyl oxygen, which leads to a qualitative difference between them and the nitrogen bases.

Experimental Section

All the mobility measurements were carried out on a Phemto-Chem 100 ion mobility spectrometer made by PCP, Inc., FL. The IMS/MS studies, to confirm the ion identities, were carried out on the MMS-160, at PCP. The experimental procedures were described in detail elsewhere.[3,10] The reduced mobilities were measured at a temperature of 200 °C, with the electric field strength set at 200 and 57 V/cm, in air and helium, respectively. The flow rates of purified and dried carrier and drift gases were set at 100 and 500 mL/min, respectively. The spectra were acquired and averaged by Computerscope hardware and software package (made by RC Electronic) interfaced to an IBM-PC/XT computer. Sample introduction was made by inserting a syringe needle, on which headspace vapors were adsorbed, into the orifice of the IMS cell. Special care was taken to avoid saturation or overloading of the instrument.

The shutter grid was opened for 0.1 ms; thus the full width at half-maximum was about 0.25 ms. For heavy ions with long drift times, the gate was opened for 0.2 ms in order to improve the signal intensity. All samples were commercially available and were used without purification.

Estimation of Errors. The reduced mobility was calculated from the formula

$$K_0 = (d/E^*t)(273/T)(P/760) \qquad (9)$$

where d is the length of the drift region (8 cm), E the electric field strength, t the drift time of the ion, T the cell temperature (200 °C), and P the atmospheric pressure (about 720 Torr at NRCN).

Given the uncertainties in measurement of the electric field strength, cell temperature, atmospheric pressure, and especially the drift time, one would expect an error of about 2%. However, use of a standard reference compound,[10] 2,4-lutidine, taken as 1.95 cm^2 V^{-1} s^{-1}, eliminates all of the above factors but the last. Thus, the error is less than 1% or within 0.01 cm^2 V^{-1} s^{-1} of the reported value of the reduced mobility in air.

In helium there is no accepted reference ion, so that eq 9 was used throughout the work, leading to an estimated error of 2%.

Results and Discussion

In a previous study on amines,[10] it was shown that the mobility of amines, for example, depends not only on the ion mass, but also on the nature of the compound. Thus, aromatic amines have a higher reduced mobility than aliphatic isobaric amines, and compounds containing solely saturated hydrocarbon chains are less mobile than isobaric compounds with heavy atoms (oxygen and halogen). As we are interested in a more general picture of the mass-mobility correlation function, we shall try to ignore these factors (except in cases of grossly deviating results).

The results of the mobility measurements of the aliphatic amines, aromatic amines, and acetyls, first in air and then in helium, will be presented and discussed separately for each family of ions.

The Fitting Procedure. In order to fit the experimental data points with the theoretical expression, eq 7 and 8, we used a nonlinear least-square fitting program. The parameters of the fit were r_0, z, and the reduced core diameter, a^*. The values of T^* and r_m, in eq 7, were calculated from a^*, r_0, and z, using the appropriate polarizability (taken from ref 2), reduced mass and temperature. The collision cross section, Ω^*, was taken from Table 1 in ref 11.

In practice, a discrete value a^* was taken, and initial (guessed) values for r_0 and z were chosen. The parameters r_0 and z were optimized by the program to fit the experimental data points, with the minimal X^2 value. Next a^* was incremented and r_0 and z were again optimized to obtain the best fit. Thus, for each value a^* the optimal r_0 and z values were obtained. The set of parameters that gave the smallest X^2 value was used as the best fit for the

---

(11) Mason, E. A.; O'Hara, H.; Smith, F. J. *J. Phys. B., At. Mol. Phys.* **1972**, *5*, 169.

(12) Griffin, G. W.; Dzidic, I.; Carroll, D. I.; Stillwell, R. N.; Horning, E. C. *Anal. Chem.* **1973**, *45*, 1204.

(13) Karpas, Z.; Berant, Z.; Stimac, R. M., submitted for publication in *Struct. Chem.*

Table I. Acetyls in Air: Compounds, Molecular Weight, Measured Reduced Mobility (K_{exp}), Results of the Calculations of the Reduced Mobility (K_{cal}), Depth of the Interaction Potential Minimum (ϵ_0) and Its Position (r_m), and Collision Cross Sections (Ω_D), Based on the Hard-Core Potential Model with $a^* = 0.2$, $r_0 = 2.20$ Å, and $z = 0.0013$ Å/amu

		K (V s/cm^2)				
compound	MW	exptl	calcd	ϵ_0 (meV)	r_m (Å°)	Ω_D (Å^2)
acetone	58	2.33	2.30	28.6	5.16	84
methyl ethyl ketone	72	2.21	2.19	23.5	5.42	86
acetylacetone	100	2.04	1.99	17.1	5.87	90
ethyl acetoacetate	114	1.84	1.90	14.9	6.07	93
acetophenone	120	1.88	1.87	14.1	6.16	94
acetylpyridine	121	1.91	1.87	14.0	6.17	94
acetylcyclopentanone	126	1.83	1.84	13.4	6.24	95
acetylcyclohexanone	140	1.74	1.77	11.9	6.43	98
trimethylacetophenone	162	1.60	1.65	10.0	6.71	103
dimethoxyacetophenone	180	1.61	1.59	8.8	6.93	107
trimethoxyacetophenone	210	1.49	1.47	7.2	7.28	114

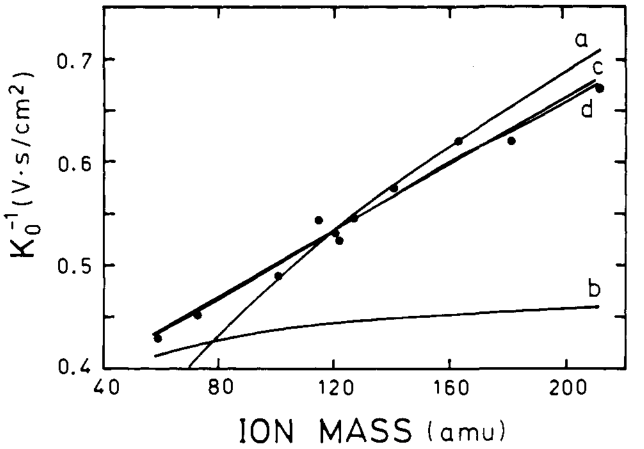

Figure 1. The measured inverse mobility, at 200 °C in air, of substituted acetyl ions as a function of ion mass. Curve a was calculated according to the rigid sphere model with $r_0 = 2.60$ Å; curve b according to the polarization limit model; curve c according to the hard-core model with $a^* = 0.2$, $z = 0$ Å/amu, and $r_0 = 2.40$ Å; and curve d with $a^* = 0.2$, $z = 0.0013$ Å/amu, and $r_0 = 2.20$ Å.

data. Similarly, a fit was obtained for the uncorrected model by setting z to zero. The solid lines in Figures 1–5 depict the calculated inverse reduced mobility obtained by use of these parameters, while the symbols represent the experimental data points.

Calculating the reduced mobility from the polarization limit model was done according to eq 4, substituting the appropriate reduced mass and polarizability. The reduced mobility values according to the rigid sphere model were calculated from eq 7, taking the collision cross section from eq 3, and using eq 6 to obtain the sum of the radii of the ion and neutral.

1. Acetyls. The mobility of the major ion formed in several compounds sharing a common acetylic functional group, CH_3CO, was determined. As shown in Table I, some of these compounds are aliphatic and some aromatic, some contain only one oxygen atom and some as many as four such atoms, and these compounds vary in size and mass from acetone (58 amu) to 2,4,6-trimethoxyacetophenone (210 amu). All these compounds have relatively high proton affinities,[14] and, based on our IMS/MS measurements and on other work,[15] it was assumed that the major ion formed in the IMS is the protonated molecule.

The measured reduced mobility in air of the major ion from each compound and the mobility calculated from the hard-core model, applying the correction introduced in eq 8, are shown in Table I. The calculated depth of the minimum in the interaction potential, ϵ_0, the separation of the ion and molecule at that point, r_m, and the collision cross sections, Ω_D, are also shown. These values were calculated using the reduced core diameter, $a^* = 0.2$, which gave the best fit with the experimental data.

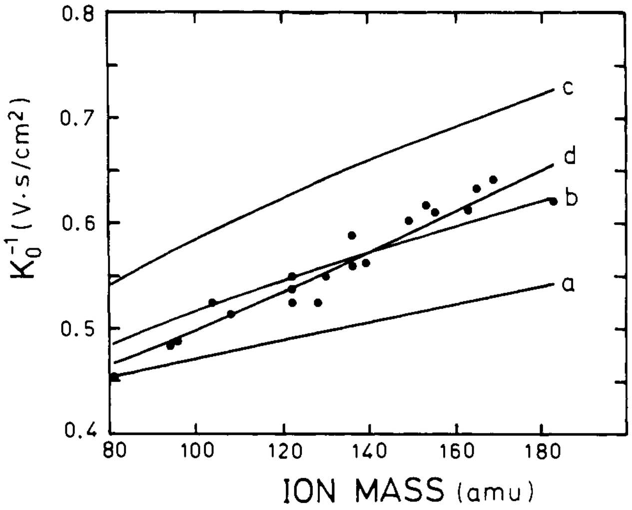

Figure 2. The measured inverse mobility, at 200 °C in air, of protonated aromatic amines as a function of ion mass. Curves a, b, and c were calculated according to the model with the hard-core potential with $a^* = 0.2$, $z = 0$ Å/amu, and r_0 values of 2.11, 2.41, and 2.71 Å, respectively. Curve d was calculated according to the corrected hard-core model with $a^* = 0.2$, $z = 0.0022$ Å/amu, and $r_0 = 2.11$ Å.

It is necessary to emphasize that the calculated values of r_m, Ω_D, and ϵ_0 given in Table I (and subsequently in Tables II and III) are the weighted average for a mixture of 80% nitrogen and 20% oxygen, taken to represent the composition of air.

In Figure 1 the experimental data for the inverse of the reduced mobility in air, at 200 °C, as a function of the acetyl ion mass, are presented. The solid lines represent the calculated inverse mobility for the rigid sphere model (curve a) and the polarization limit model (curve b). Curves c and d are the fits obtained by using the hard-core model (eq 5 and 7). In curve c, the parameter z was set to zero and the parameters obtained from the fitting procedure were $r_0 = 2.40$ Å and $a^* = 0.2$. In curve d, z was also optimized by the fitting procedure, and the values obtained for r_0, z, and a^* were 2.20 Å, 0.0013 Å/amu, and 0.2, respectively. Evidently, the polarization limit approximation fails to reproduce the results quantitatively, and even the qualitative representation is poor. The rigid sphere model did somewhat better quantitatively over a limited range of ion masses. On the other hand, the hard-core model for large polyatomic ions[3] gives quite a good quantitative reproduction of the measured data, well within 5% of the experimental values. This is reasonable, especially when one considers the variety in nature, size, and shape of the ions.

The contribution of the correction factor, z, to achieving a better fit is quite small as expressed by its lower X^2 value in this series of acetyl compounds, but its importance will become evident in the next sections.

---

(14) Lias, S. G.; Liebman, J. F.; Levin, R. D. *J. Phys. Chem. Ref. Data* **1984**, *13*, 695.

(15) Benezra, S. A. *J. Chromatogr. Sci.* **1976**, *14*, 122.

(16) Karasek, F. W.; Kim, S. H.; Rokushika, S. *Anal. Chem.* **1978**, *50*, 2013.

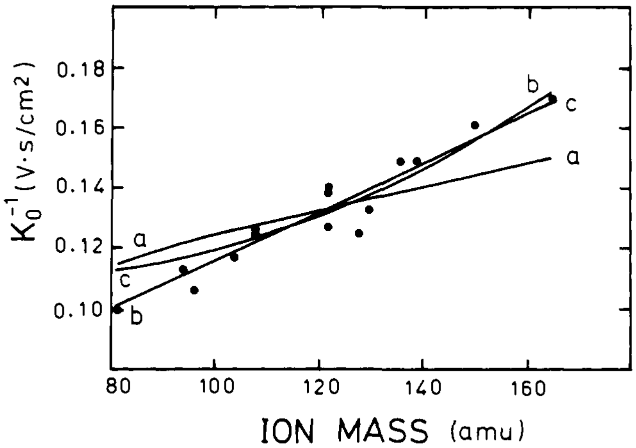

Figure 3. The measured inverse mobility, at 200 °C in helium, of protonated aromatic amines as a function of ion mass. Curve a was calculated according to the model with the hard-core potential with $a^* = 0.1$, $z = 0$ Å/amu, and $r_0 = 1.51$ Å; curve b with $a^* = 0.1$, $z = 0.0031$ Å/amu, and $r_0 = 1.13$ Å; and curve c with $a^* = 0.4$, $z = 0.0039$ Å/amu, and $r_0 = 0.599$ Å.

2. Aromatic Amines. Aromatic amines, pyridines and anilines, differ qualitatively from the acetyls in two major aspects. The carbon skeleton of the molecule, the aromatic system, is more rigid, and the site of protonation is on nitrogen (or in some anilines on carbon[13]) rather than on oxygen. The points in Figure 2 show the inverse of the measured reduced mobility in air as a function of the ion mass. Curves a, b, and c were calculated from eq 5 and 7, with $z = 0$, $a^* = 0.2$, and r_0 values of 2.11, 2.41, and 2.71 Å, respectively. Curve d was obtained from the fitting procedure with $a^* = 0.2$, $z = 0.0022$ Å/amu, and $r_0 = 2.11$ Å. The sensitivity of the calculation to the choice of r_0 is clearly demonstrated here, as even small changes in r_0 shift the curve considerably. The inclusion of the correction factor, z (curve d), improved the fit with the experimental data points.

Figure 3 shows the mobility measurements of aromatic amines in helium. The reduced mobility of a given ion in helium is higher by a factor of about 4 than in air (Table II). This arises from the difference in the reduced mass and from the difference in polarizability of helium and air, which are 0.205×10^{-24} and 1.73×10^{-24} cm³ (weighted average of nitrogen and oxygen), respectively (Appendix 2 of ref 2). This leads to a much weaker attractive interaction between the ion and helium (see ϵ_0 values in Table II). The mass dependence of the inverse reduced mobility in helium is more prominent than in air. Therefore, taking $a^* = 0.1$ and $r_0 = 1.51$ Å and setting $z = 0$ (curve a) fail to reproduce the experimental data quantitatively, while calculations including the correction term did quite well as curves b and c in Figure 3 demonstrate. Curve b was obtained with $a^* = 0.1$, $z = 0.0031$ Å/amu, and $r_0 = 1.13$ Å and curve c with $a^* = 0.4$, $z = 0.0039$ Å/amu, and $r_0 = 0.599$ Å. Note the relatively small effect that the choice of a^* has on the curve fitting for mobility measurements in helium, which will be discussed below.

It is also interesting to compare the depth of the interaction potential minimum, ϵ_0, and the collision cross section, Ω_D, in both drift gases (Table II). For a given ion, ϵ_0 is an order of magnitude larger in air than in helium and Ω_D is about twice as large. These are manifestations of the much stronger attractive interaction between the ion and the air (nitrogen and oxygen) molecules, compared with helium, which arise from the polarizability difference between the drift gases.

3. Aliphatic Amines. Aliphatic amines resemble the aliphatic acetyls more than do the aromatic compounds described above, as they have no rigid skeleton, and only a relatively small functional group. The masses of the ions (from 32 to 522 amu, Table III) in this family of compounds span a wider range than in the other families of compounds. Furthermore, as this group contains primary, secondary, and tertiary amines, as well as normal and branched compounds, it can serve as the most rigorous test case for the mobility theories.

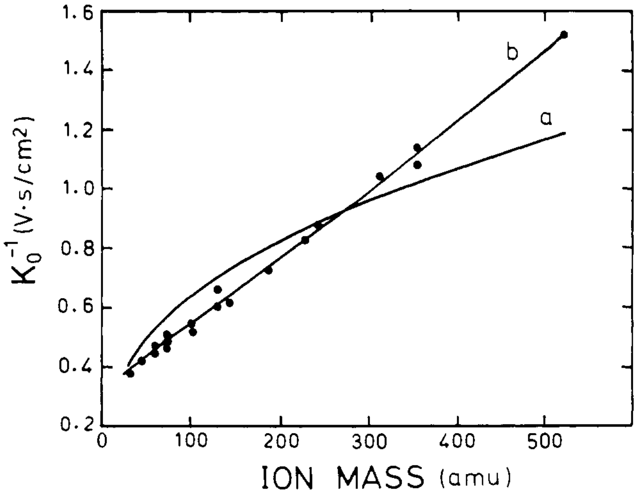

Figure 4. The measured inverse mobility, at 200 °C in air, of protonated aliphatic amines as a function of ion mass. Curve a was calculated according to the hard-core model with $a^* = 0.2$, $z = 0$ Å/amu, and $r_0 = 2.89$ Å; curve b with $a^* = 0.2$, $z = 0.0021$ Å/amu, and $r_0 = 2.34$ Å.

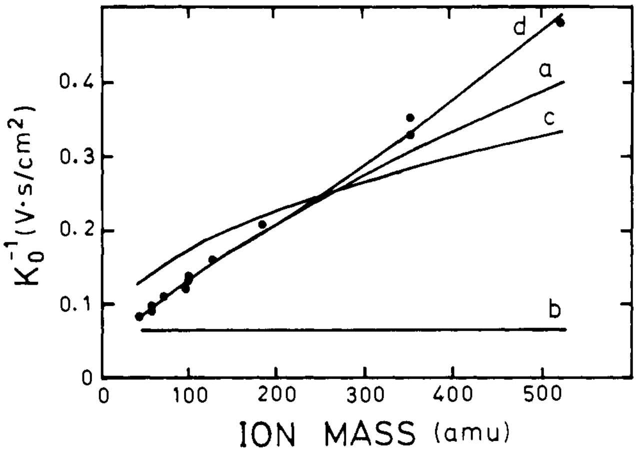

Figure 5. The measured inverse mobility, at 200 °C in helium, of protonated aliphatic amines as a function of ion mass. Curve a was calculated according to the rigid sphere model ($r_0 = 1.80$ Å); curve b according to the polarization limit model; curve c according to the hard-core model with $a^* = 0.1$, $z = 0$ Å/amu, and $r_0 = 1.91$; curve d with $a^* = 0.1$, $z = 0.0022$ Å/amu, and $r_0 = 1.36$.

Figure 4 depicts the inverse reduced mobility in air as function of the ion mass. Curve a shows the calculated mobility with the correction factor set to zero, $a^* = 0.2$, and $r_0 = 2.89$ Å and in curve b $a^* = 0.2$, $z = 0.0021$ Å/amu, and $r_0 = 2.34$ Å.

In Figure 5 the inverse reduced mobility in helium is shown as a function of ion mass. Curve a was obtained with the rigid sphere model and curve b with the polarization limit model. The model with the hard-core potential was used to obtain curves c and d. In curve c the parameters were $a^* = 0.1$, $z = 0$, and $r_0 = 1.91$ Å°, and in curve d $a^* = 0.1$, $z = 0.0022$ Å/amu, and $r_0 = 1.36$ Å.

In air, and especially in helium, the mobility calculated with polarization limit model deviates considerably from the experimental data points, while the rigid sphere and the uncorrected hard-core potential models reproduce the data only over a limited mass range. On the other hand, the hard-core model with the correction factor reproduced the experimental values to within 5% in both drift gases over the entire mass range.

The value of z in helium and in air is about the same, but its importance in helium is significantly greater, as its relative effect on r_m is larger. Here too, as seen in Table III, the reduced mobility of ions in helium is larger by a factor of 5 for light ions and of 3 for heavy ions than in air. Once more, for a given ion, the calculated interaction potential, ϵ_0, in air is an order of magnitude larger than in helium, while the r_m values are within 25% of one

Table II. Aromatic Amines in Air and in Helium: Compounds, Molecular Weight, Measured Reduced Mobility (K_{exp}), Results of the Calculations of the Reduced Mobility (K_{cal}), Depth of the Interaction Potential Minimum (ϵ_0) and Its Position (r_m), and Collision Cross Sections (Ω_D), Based on the Hard-Core Potential Model[a]

		air					helium				
		K (V s/cm^2)					K (V s/cm^2)				
compound	MW	exptl	calcd	ϵ_0 (meV)	r_m (Å)	Ω_D (Å^2)	exptl	calcd	ϵ_0 (meV)	r_m (Å)	Ω_D (Å^2)
pyridine	79	2.21	2.15	22.7	5.47	86	10.1	10.0	2.2	5.09	43
3-picoline	93	2.07	2.04	18.9	5.72	88	8.87	9.01	1.7	5.47	48
aniline	93	2.07	2.04	18.9	5.72	88	8.84	9.01	1.7	5.47	48
3-hydroxypyridine	95	2.06	2.03	18.4	5.76	89	9.44	8.90	1.6	5.53	49
3-cyanopyridine	104	1.91	1.98	16.8	5.90	91	8.54	8.47	1.4	5.74	52
3-toluidine	107	1.95	1.95	16.0	5.97	91	7.99	8.20	1.3	5.84	53
2,4-lutidine	107	1.95	1.95	16.0	5.97	91	7.92	8.20	1.3	5.84	53
2-acetylpyridine	121	1.91	1.86	13.7	6.20	95	7.87	7.50	1.0	6.21	58
2,4,6-collidine	121	1.82	1.86	13.7	6.20	95	7.13	7.50	1.0	6.21	58
3,5-dimethylaniline	121	1.86	1.86	13.7	6.20	95	7.21	7.50	1.0	6.21	58
2-chloroaniline	127	1.91	1.82	12.9	6.30	96	8.02	7.25	0.9	6.37	60
quinoline	129	1.82	1.81	12.6	6.33	97	7.52	7.14	0.9	6.42	60
4-*tert*-butylpyridine	135	1.70	1.77	11.9	6.43	98					
4-acetylaniline	135	1.79	1.77	11.9	6.43	98	6.73	6.90	0.8	6.57	62
3-nitroaniline	138	1.78	1.75	11.5	6.47	99	6.69	6.78	0.8	6.65	64
N,*N*-diethylaniline	149	1.66	1.70	10.5	6.63	102	6.21	6.38	0.7	6.94	68
2,4-dimethoxyaniline	153	1.62	1.68	10.1	6.69	103					
2-phenylpyridine	155	1.64	1.66	10.0	6.72	103					
2,5-dichloroaniline	163	1.63	1.62	9.2	6.85	106					
4-amino-*N*,*N*-diethylaniline	164	1.58	1.61	9.1	6.88	106	5.88	5.89	0.5	7.32	73
diphenylamine	169	1.56	1.59	8.7	6.94	107					
2,4-dinitroaniline	183	1.61	1.52	7.8	7.15	112					

[a] The fit parameters were $a^* = 0.2$, $r_0 = 2.11$ Å, and $z = 0.0022$ Å/amu, in air and $a^* = 0.1$, $r_0 = 1.13$ Å, and $z = 0.0031$ Å/amu, in helium.

Table III. Aliphatic Amines in Air and in Helium: Compounds, Molecular Weight, Measured Reduced Mobility (K_{exp}), Results of the Calculations of the Reduced Mobility (K_{cal}), Depth of the Interaction Potential Minimum (ϵ_0) and Its Position (r_m), and the Collision Cross Sections (Ω_D), Based on the Hard-Core Potential Model[a]

		air					helium				
		K (V s/cm^2)					K (V s/cm^2)				
compound	MW	exptl	calcd	ϵ_0 (meV)	r_m (Å)	Ω_D (Å^2)	exptl	calcd	ϵ_0 (meV)	r_m (Å)	Ω_D (Å^2)
methylamine	31	2.65	2.63	35.7	4.88	83					
ethylamine	45	2.38	2.39	26.4	5.27	84	12.1	11.3	3.0	4.74	39
trimethylamine	59	2.36	2.21	20.7	5.59	87	10.6	10.0	2.1	5.15	44
isopropylamine	59	2.36	2.21	20.7	5.59	87	10.5	10.0	2.1	5.15	44
n-propylamine	59	2.36	2.21	20.7	5.59	87	10.4	10.0	2.1	5.15	44
1,2-diaminoethane	60	2.25	2.20	20.4	5.62	87	11.0	9.9	2.1	5.18	44
diethylamine	73	2.15	2.06	16.9	5.89	90	9.1	9.0	1.6	5.53	49
isobutylamine	73	2.02	2.06	16.9	5.89	90	9.1	9.0	1.6	5.53	49
n-butylamine	73	1.98	2.06	16.9	5.89	90	9.1	9.0	1.6	5.53	49
cyclohexylamine	99	1.83	1.84	12.2	6.38	97	8.2	7.6	1.0	6.17	57
triethylamine	101	1.95	1.82	11.9	6.42	98	7.6	7.5	1.0	6.22	60
di-*n*-propylamine	101	1.87	1.82	11.9	6.42	98	7.3	7.5	1.0	6.22	60
diisobutylamine	129	1.66	1.64	9.0	6.98	107	6.2	6.5	0.7	6.87	66
n-octylamine	129	1.51	1.64	9.0	6.98	107					
tri-*n*-propylamine	143	1.63	1.56	7.9	7.13	111					
tri-*n*-butylamine	185	1.38	1.36	5.5	7.77	125	4.8	5.1	0.4	8.09	84
tri-*n*-pentylamine	227	1.21	1.21	3.7	8.39	139					
n-hexadecylamine	241	1.14	1.16	3.7	8.59	144					
tri-*n*-heptylamine	311	0.96	0.98	2.4	9.56	168					
triisooctylamine	353	0.93	0.90	1.9	10.13	183	3.0	3.0	0.1	11.6	142
tri-*n*-octylamine	353	0.88	0.90	1.9	10.13	183	2.8	3.0	0.1	11.6	142
tri-*n*-dodecylamine	521	0.66	0.65	0.9	12.37	247	2.1	2.0	.03	15.1	209

[a] The fit parameters were $a = 0.2$, $r_0 = 2.11$ Å, and $z = 0.0021$ Å/amu, in air and $a^* = 0.1$, $r_0 = 1.12$ Å, and $z = 0.0032$ Å/amu, in helium.

another. However, the range of variation of r_m is larger in helium than in air, so that, while for light ions it is smaller in helium, for the heavy ions r_m in helium is actually larger than in air.

Selection of a homologous series of normal tertiary aliphatic amines can serve as a good test for the models. Figure 6 depicts the inverse reduced mobility of these ions in air at 200 °C. Curve a is calculated according to the polarization limit, curve b according to the rigid sphere model; curve c is the hard-core model with z set to zero; and curve d is the corrected model. Even in this homologous series, the addition of the correction factor greatly improves the fit with the experimental data, particularly for ions above mass 200 amu. It is interesting to note that while $a^* = 0.2$ gave the best fit when all the aliphatic amines were accounted for (Figure 4), for the normal tertiary amines alone, a slightly better fit was obtained for $a^* = 0.1$ (Figure 6). This could be an indication that the separation of the center of charge and center of mass in tertiary amines is smaller than in primary amines, as expected intuitively from assuming that the charge is largely localized on the nitrogen atom.

Summary and Conclusions

In order to summarize and emphasize some of the points made above, we shall try to look at the overall picture emerging from the data.

The depth of the minimum in the ion–neutral interaction potential, ϵ_0, the distance between them at that point, r_m, and the collision cross section, Ω_D, were calculated on the basis of the model employing a hard-core potential with the correction factor (see

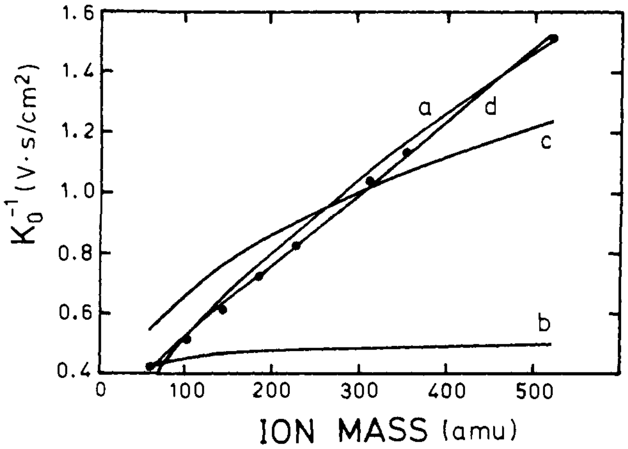

Figure 6. The measured inverse mobility, at 200 °C in air, of a homologous series of protonated normal tertiary aliphatic amines as a function of ion mass. Curve a was calculated according to the rigid sphere model (r_0 = 4.1 Å); curve b according to the polarization limit model; curve c according to the hard-core model with $a^* = 0.1$, $z = 0$ Å/amu, and r_0 = 3.31 Å; and curve d with $a^* = 0.1$, $z = 0.0025$ Å/amu, and r_0 = 2.53 Å.

Tables I–III). These calculated values depend on a^*, as evident from eq 5. In air, the curve-fitting procedure is strongly dependent on the choice of a^*, with $a^* = 0.2$ giving the best fit. The quality of the fit diminishes by changing a^*. In the acetyls (Figure 1), aromatic amines (Figure 2), and all aliphatic amines (Figure 4), taking $a^* = 0.2$ gave the best fit (as expressed by X^2), while in the normal tertiary amines (Figure 6) a somewhat better fit was obtained with $a^* = 0.1$. In helium, variation of a^* from 0 to 0.3 barely affected the quality of the fit, while taking $a^* = 0.4$ had only a small effect (Figure 3).

As mentioned above, the values of r_m and Ω_D, and especially of ϵ_0, depend strongly on the choice of a^*. Therefore, as the purely mathematicaly fitting procedure is insensitive to variation of a^*, it must be selected from physical considerations. There is no experimental data from other techniques, except IMS, on the strength of the ion–helium interaction. The fact that the attractive interaction of a given ion with helium is weaker than in air is an indication on the choice of a^*. Thus, taking a large value (a^* = 0.4) for helium would yield an unreasonably large calculated interaction potential; therefore, $a^* = 0.1$ was chosen for helium.

In conclusion, it appears that taking $a^* = 0.2$ for ions in air and $a^* = 0.1$ in helium is an a priori reasonable choice for these ions in all cases. It is especially interesting to compare the collision cross sections. First, the values obtained are in good agreement with those reported by Hagen.[17] Second, evidently the collision cross section for a given ion in helium is about half that in air.

Finally, one can use the rigid sphere approximation to calculate the radius of the ion (from the sum of radii). For protonated pyridine, for example, the result would be about 3.8 Å, which reasonably agrees with the ab initio calculations of Del-Bene.[18] Thus, although this approximation poorly reproduces mobility results, it can give a crude estimate of the ion radius once the collision cross section has been derived from the mobility measurements. Comparison of the results obtained for Ω_D, r_m, and ϵ_0 for ions drifting through helium and through air gives an insight as to the differences in the ion–neutral interactions. For a given ion, the collision cross section is about double the size in air than in helium, which reflects the relative size of the neutral species. The depth of the minimum (ϵ_0) in the interaction potential is smaller in helium by an order of magnitude, while r_m differs by less than 25%. The difference in size between helium atoms and the air (nitrogen and oxygen) molecules, which causes the collision cross-section differences, also partly accounts for the somewhat smaller r_m in helium. On the other hand, the difference between the polarizability of helium and of air leads to a much weaker attractive interaction between the ion and helium atoms. Thus, the difference in size leads to a smaller collision cross section in helium, and the polarizability difference leads to a stronger interaction of the ion with air, resulting in mobilities in helium that are higher by a factor of 3–5 than in air.

The introduction of the correction factor, z, enhanced the agreement between the measured data points and the calculations based on the hard-core model. This improvement was evident especially for the mobility measurements of polyatomic ions in helium and for mobility measurements of ions with masses above 200 amu, in air. As most of the earlier studies were concerned with a limited mass range of ions, and with air or nitrogen as drift gases, the problem of a quantitative fit was not as severe and did not arise.

Registry No. He, 7440-59-7.

---

[17] Hagen, D. F. In *Plasma Chromatography*; Carr, T. W., Ed.; Plenum Press: New York, 1984; Chapter 4.

[18] Del-Bene, J. E. *J. Am. Chem. Soc.* **1975**, *97*, 5330.

Direct Measurement of the Enthalpy Difference between Enol and Keto Forms by the Time-Resolved Thermal Lens Method: 7-Hydroxyquinoline

Masahide Terazima* and Tohru Azumi

Contribution from the Department of Chemistry, Faculty of Science, Tohoku University, Sendai, 980, Japan. *Received September 6, 1988*

Abstract: The enthalpy difference between the keto and enol forms of 7-hydroxyquinoline is measured by using the time-resolved thermal lens technique. The obtained large difference, 3400 cm^{-1}, in the ground state and −4200 cm^{-1} in the excited singlet state indicate the predominant enol form in the ground state and keto form in the excited state.

1. Introduction

A protropic tautomerism of heteroaromatic compounds containing a hydroxy group at the excited state has long been of interest to chemists and has attracted further attention in recent years. For such molecules, electronic excited states of keto and enol forms have been investigated extensively by using absorption and/or emission spectroscopy.[1-7] Although the enthalpy difference (ΔH) between the keto and enol forms is one of the important

---

[1] Huppert, D.; Gutman, M.; Kaufmann, K. J. In *Photoselective Chemistry*; Jortner, J., Levine, R. D., Rice, S. A., Eds.; Wiley: New York, 1981; Vol. 2.

0002-7863/89/1511-3824$01.50/0